

Impact of spontaneously emitted photon on the dynamic behaviors of injection-locked semiconductor lasers

YUQING FU*, JIANGUO CHEN

Department of Optoelectronics, Sichuan University, Chengdu, 610064, China

*Corresponding author: yuqingfu841126@yahoo.com.cn

Starting from the mean-field rate equations describing the dynamic behaviors of the slave laser (SL) in the injection-locked master-slave semiconductor laser system (MSL), applying the perturbation method and the Cardan formula, analytical solutions to the evolutions of perturbations from the fixed point have been derived. The dynamic behaviors of the SL perturbed by a spontaneously emitted photon have been analyzed by using the above solutions. Finally, the phase space portraits with different phase between the spontaneously emitted photon and the injection field have also been investigated.

Keywords: injection-locked master-slave semiconductor laser, fixed point, dynamic behavior, phase space portrait, spontaneously emitted photon, analytical solution.

1. Introduction

Since the 1980s, intensified studies have been made on the injection-locked master-slave semiconductor laser systems (MSLs) [1]. These studies include bandwidth modulation, noise and stability analyzes, *etc.* [2–4]. In fact, the MSLs are used not only to improve the beam quality of the slave laser (SL) [5] and enhance the cavity frequency, *etc.* [6], but also to provide an ideal physical platform for the nonlinear dynamic physics [7–14]. At present, chaotic semiconductor laser systems and traditional communication technologies may be combined, making the chaotic communication become an important branch in modern communications [15–18]. From the reports on the MSLs, it can be realized that most studies did not consider the impact of the spontaneous emission, which are applicable to the case when the contribution of injection light is much greater than that of the spontaneous emission. In other words, the spontaneous emission was categorized as certain sorts of disturbance. Meanwhile, when the perturbation method is used to analyze the dynamic behavior of a nonlinear system, one often assumes that some unknown disturbance makes the system deviate from its steady state. In this work, we specify the physical

cause of disturbance, *i.e.*, a spontaneously emitted photon, to carry out the studies on the dynamic behaviors of the slave laser in the MSLs.

2. Theoretical analysis

2.1. Rate equations and analytical solutions to the fixed point of a MSL

The injection-locked system consists of a master laser (ML) and a slave laser (SL). An isolator is placed between these two lasers to guarantee the unidirectional propagation of the light from the ML to the SL. The mean-field rate equations describing the dynamic behaviors of the SL are as follows [19]:

$$\frac{dA(t)}{dt} = \frac{1}{2} g [N(t) - N_{\text{th}}] A(t) + \frac{KA_{\text{sol}}}{\tau_L \cos[\phi(t)]} \quad (1a)$$

$$\frac{d\phi(t)}{dt} = \frac{1}{2} \alpha g [N(t) - N_{\text{th}}] - \frac{KA_{\text{sol}} \sin[\phi(t)]}{\tau_L A(t)} - \Delta\omega \quad (1b)$$

$$\frac{dN(t)}{dt} = \frac{N_p - N(t)}{\tau_s} - \left\{ \frac{1}{\tau_p} + g [N(t) - N_{\text{th}}] \right\} A^2(t) \quad (1c)$$

where $A^2(t)$ and $N(t)$ represent the photon and carrier densities, respectively; g is the differential gain coefficient; A_{sol}^2 and N_{th} are, respectively, the photon and threshold carrier densities of the free-running SL; $K = A_{\text{inj}}^2 / A_{\text{sol}}^2$, with K^2 being the so-called the injection coefficient, A_{inj}^2 is the photon density injected into the SL; τ_L is the round-trip time inside the SL cavity; $\phi(t)$ is the phase difference, $\phi_m(t) - \phi_s(t)$, between the master and slave fields; $\Delta\omega$ is the angular frequency difference, $\omega_m - \omega_s$, between the master and slave fields; α is the linewidth enhancement factor; N_p is the carrier density created by the pump current; τ_s and τ_p are the lifetimes of the carriers and photons, respectively.

In the steady state, the photon density A_{st}^2 , the phase difference ϕ_{st} between the master and slave fields, and the carrier density N_{st} satisfy the following equations

$$\frac{1}{2} g (N_{\text{st}} - N_{\text{th}}) A_{\text{st}} + k A_{\text{sol}} \cos(\phi_{\text{st}}) = 0 \quad (2a)$$

$$\frac{1}{2} \alpha g (N_{\text{st}} - N_{\text{th}}) - \frac{k A_{\text{sol}} \sin(\phi_{\text{st}})}{A_{\text{st}}} - \Delta\omega = 0 \quad (2b)$$

$$\frac{N_p - N_{\text{st}}}{\tau_s} - \left[\frac{1}{\tau_p} + g (N_{\text{st}} - N_{\text{th}}) \right] A_{\text{st}}^2 = 0 \quad (2c)$$

where k stands for K/τ_L . In Equation (2), A_{st}^2 , ϕ_{st} and N_{st} are the three quantities to be solved. By using the above equations, one can obtain

$$G_a G^3 + G_b G^2 + G_c G + G_d = 0 \quad (3)$$

where:

$$G_a = 1 + \alpha^2$$

$$G_b = -\left(\frac{g\Delta N G_a}{2} + 2\alpha\Delta\omega\right)$$

$$G_c = g\alpha\Delta N\Delta\omega + \Delta\omega^2 + k^2$$

$$G_d = g\Delta N \frac{k^2 - \Delta\omega^2}{2}$$

$$G = \frac{g(N_{st} - N_{th})}{2}$$

$$\Delta N = N_p - N_{th}$$

Equation (3) is a cubic equation about G and its analytical solutions can be derived by using the Cardan formula. Once the quantity G is obtained, the expressions for the fixed point parameters of the SL can be obtained, which read

$$N_{st} = \frac{2G}{g} + N_{th} \quad (4a)$$

$$A_{st}^2 = \frac{A_{sol}^2(1 - 2G\tau_p)}{1 + 2G\tau_p} \quad (4b)$$

$$\cos(\phi_{st}) = -\frac{GA_{st}}{kA_{sol}} \quad (4c)$$

2.2. The dynamic behaviors in the proximity of fixed points

In this section, we will analyze the dynamic behaviors of how a MSL system evolves from an initial state in the proximity of the fixed point to the fixed state. If the initial state is close to the fixed point, the parameters of the SL can be expressed as the sum of the steady state parameters and the deviations, which are

$$X(t) = X_{st} + \delta X(t), \quad X = A, \phi, N \quad (5)$$

If the initial state is close enough to the fixed point, then the perturbation method [19] can be used to deal with this situation. Substituting Eq. (5) into Eq. (1) and neglecting the higher order small quantities (*i.e.*, the square of the small changes, the cross-product terms as well as the higher order terms), the first order linear differential equations describing the dynamic behavior in the vicinity of the fixed point can be obtained, which are

$$\begin{bmatrix} \delta \dot{A}(t) \\ \delta \dot{\phi}(t) \\ \delta \dot{N}(t) \end{bmatrix} = \begin{pmatrix} a_{11} & a_{12} & a_{13} \\ a_{21} & a_{22} & a_{23} \\ a_{31} & a_{32} & a_{33} \end{pmatrix} \begin{bmatrix} \delta A(t) \\ \delta \phi(t) \\ \delta N(t) \end{bmatrix} \quad (6)$$

where $a_{11} = G$, $a_{12} = -kA_{\text{sol}}\sin(\phi_{\text{st}})$, $a_{13} = gA_{\text{st}}/2$, $a_{21} = kA_{\text{sol}}\sin(\phi_{\text{st}})/A_{\text{st}}^2$, $a_{22} = -kA_{\text{sol}}\cos(\phi_{\text{st}})/A_{\text{st}}$, $a_{23} = g\alpha/2$, $a_{31} = -2A_{\text{st}}(1/\tau_p + 2G)$, $a_{32} = 0$, $a_{33} = -(1/\tau_s + gA_{\text{st}}^2)$.
Let

$$\delta X(t) = \delta X_0 \exp(\lambda t), \quad X = A, \phi, N \quad (7)$$

where δX_0 represents the deviations from the fixed point at the initial moment $t = 0$. Substituting Eq. (7) into Eq. (6), one can obtain the following equations that the initial deviations should satisfy

$$\begin{cases} (a_{11} - \lambda)\delta A_0 + a_{12}\delta\phi_0 + a_{13}\delta N_0 = 0 \\ a_{21}\delta A_0 + (a_{22} - \lambda)\delta\phi_0 + a_{23}\delta N_0 = 0 \\ a_{31}\delta A_0 + a_{32}\delta\phi_0 + (a_{33} - \lambda)\delta N_0 = 0 \end{cases} \quad (8)$$

Equation (8) is a homogeneous linear equation, and the condition that Eq. (8) has non-trivial solution is

$$\begin{vmatrix} a_{11} - \lambda & a_{12} & a_{13} \\ a_{21} & a_{22} - \lambda & a_{23} \\ a_{31} & a_{32} & a_{33} - \lambda \end{vmatrix} = 0 \quad (9)$$

Equation (9) is a cubic equation. Its three roots $\lambda_1, \lambda_2, \lambda_3$ can be obtained by using the Cardan formula. For a stable fixed point, the real part of the above three roots should all be negative.

As λ satisfies Eq. (9), only two equations of Eq. (8) are independent. In other words, from Eq. (8), one can use one parameter to express the other two parameters. Given δA_0 , one can find

$$\delta\phi_0(\lambda_j) = \frac{\begin{vmatrix} \lambda_j - a_{11} & a_{13} \\ -a_{21} & a_{23} \end{vmatrix}}{\begin{vmatrix} a_{12} & a_{13} \\ a_{22} - \lambda_j & a_{23} \end{vmatrix}} \delta A_0 \equiv f_j \delta A_0, \quad j = 1, 2, 3 \quad (10a)$$

$$\delta N_0(\lambda_j) = \frac{\begin{vmatrix} \lambda_j - a_{11} & a_{12} \\ a_{21} & \lambda_j - a_{22} \end{vmatrix}}{\begin{vmatrix} a_{12} & a_{13} \\ a_{22} - \lambda_j & a_{23} \end{vmatrix}} \delta A_0 \equiv h_j \delta A_0, \quad j = 1, 2, 3 \quad (10b)$$

where f_j, h_j are functions of λ_j . The solutions of the differential equations (6) are

$$\begin{cases} \delta A = d_1 \exp(\lambda_1 t) + d_2 \exp(\lambda_2 t) + d_3 \exp(\lambda_3 t) \\ \delta\phi = f_1 d_1 \exp(\lambda_1 t) + f_2 d_2 \exp(\lambda_2 t) + f_3 d_3 \exp(\lambda_3 t) \\ \delta N = h_1 d_1 \exp(\lambda_1 t) + h_2 d_2 \exp(\lambda_2 t) + h_3 d_3 \exp(\lambda_3 t) \end{cases} \quad (11)$$

where d_1, d_2 and d_3 are constants that can be specified by using the initial deviations $\delta A_0, \delta\phi_0$ and δN_0 . Substituting the initial deviations into Eq. (11), one finds

$$d_1 = \frac{\begin{vmatrix} \delta A_0 & 1 & 1 \\ \delta\phi_0 & f_2 & f_3 \\ \delta N_0 & h_2 & h_3 \end{vmatrix}}{\Delta} \quad (12a)$$

$$d_2 = \frac{\begin{vmatrix} 1 & \delta A_0 & 1 \\ f_1 & \delta\phi_0 & f_3 \\ h_1 & \delta N_0 & h_3 \end{vmatrix}}{\Delta} \quad (12b)$$

$$d_3 = \frac{\begin{vmatrix} 1 & 1 & \delta A_0 \\ f_1 & f_2 & \delta\phi_0 \\ h_1 & h_2 & \delta N_0 \end{vmatrix}}{\Delta} \quad (12c)$$

where

$$\Delta = \begin{vmatrix} 1 & 1 & 1 \\ f_1 & f_2 & f_3 \\ h_1 & h_2 & h_3 \end{vmatrix} \quad (13)$$

Now, we can say that the dynamic behaviors of the SL from a perturbed initial state in the proximity of a fixed point to the fixed state have been completely determined. Even though, we still want to add a few words on these solutions. Since δX ($X=A, \phi, N$) are physical quantities, the solutions should be real numbers. For the case when λ_3 is a real number, and λ_1 and λ_2 satisfy

$$\lambda_1 = \lambda_2^* = \lambda_R + i\lambda_I \quad (14)$$

where, λ_R and λ_I are the real and imaginary parts of λ_I , respectively, and the superscript “*” represents complex conjugate. After lengthy calculations, it can be derived that

$$\delta A = 2d_R \cos(\lambda_I t) \exp(\lambda_R t) - 2d_I \sin(\lambda_I t) \exp(\lambda_R t) + d_3 \exp(\lambda_3 t) \quad (15a)$$

$$\begin{aligned} \delta \phi &= 2(f_R d_R - f_I d_I) \cos(\lambda_I t) \exp(\lambda_R t) - 2(f_R d_I + f_I d_R) \sin(\lambda_I t) \exp(\lambda_R t) + \\ &+ f_3 d_3 \exp(\lambda_3 t) \end{aligned} \quad (15b)$$

$$\begin{aligned} \delta N &= 2(h_R d_R - h_I d_I) \cos(\lambda_I t) \exp(\lambda_R t) - 2(h_R d_I + h_I d_R) \sin(\lambda_I t) \exp(\lambda_R t) + \\ &+ h_3 d_3 \exp(\lambda_3 t) \end{aligned} \quad (15c)$$

where y_R and y_I ($y = d_1, f_1, h_1$) are the real and imaginary parts of y , respectively.

From Equations (15), it can be realized that each deviation comprises three components (denoted by $\delta A_1, \delta A_2, \delta A_3$ for δA , and so on). The first two components experience damped oscillations at the same damping rate ($-\lambda_R$) and oscillation frequency (λ_I), but with a phase difference of $\pi/2$ between them. And the last component reduces to zero monotonously at another decay rate ($-\lambda_3$). From Equations (12), it can be understood that the initial magnitudes of all the nine components depend on the three initial deviations $\delta A_0, \delta \phi_0$ and δN_0 . This indicates that, even if one of the initial deviation, says δN_0 , is equal to zero, all the three components of $\delta N(t)$ are not necessarily equal to zero. The only fact is that the sum of these three components is equal to zero at the initial moment $t = 0$.

2.3. Impact of one spontaneously emitted photon on the injection-locked system

In this section, the impact of disturbances, arising from a spontaneously emitted photon, on the system is considered. As is known to all, the spontaneous emission is likely to be produced when the laser medium is relaxed from the upper level to

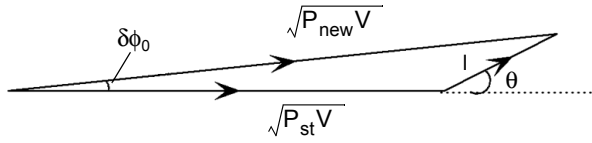


Fig. 1. The phasor diagram describing the impact of one spontaneously emitted photon on the laser field.

the lower level. A small part of this spontaneous emission is in the same mode as the laser field, and is finally coupled into the laser field. In the mean field rate equations with fixed-carrier lifetime, the contribution of spontaneous emission to the increment of the photon density is usually expressed as $\beta N_{st}/\tau_s$ [20]. Here, β is the fraction of spontaneous emission coupled to the lasing mode. For an index-guided semiconductor laser, β is a small quantity with an order of about 10^{-5} [20]. Because of this, the contribution of spontaneous emission is much smaller than that of injection light. Therefore, the contribution of spontaneous emission on the photon density is generally neglected when one discusses the characteristics of an injection-locked semiconductor laser. However, in a practical system, as the particle nature of photons, the spontaneous emission coupled into the laser mode may probably take the form of one photon. This impulse effect may be obviously larger than that from the averaged term of $\beta N_{st}/\tau_s$, and should be taken into consideration.

Since there is a large number of photons inside the SL, one can assume that the laser field is perturbed by a spontaneously emitted photon coupled into the laser mode in the SL with a phase difference of θ , at certain initial moment $t = 0$. As a result, the amplitude and phase of the laser light are perturbed to deviate from the fixed point. To determine the initial perturbation, one can use the phasor diagram shown in Fig. 1. Assume the field amplitude is proportional to the square root of the photon number. It can be realized that the field amplitude changes from $\sqrt{P_{st}V}$ to $\sqrt{P_{new}V}$ by one spontaneously emitted photon, with $P_{new} = (A_{st} + \delta A_0)^2$ and V representing the volume of the active region of the SL. Meanwhile, the phase of the laser field may also be shifted by a small quantity of $\delta\phi_0$, as shown in Fig. 1.

Using the cosine theorem, one can prove that

$$P_{new} = P_{st} + 2\sqrt{\frac{P_{st}}{V}} \cos \theta + \frac{1}{V} \quad (16)$$

Applying the sine theorem, one finds that

$$\delta\phi_0 = \text{asin} \left(\frac{\sin \theta}{\sqrt{P_{new}V}} \right) \quad (17a)$$

and

$$\delta A_0 = \sqrt{P_{new}} - \sqrt{P_{st}} \quad (17b)$$

Since the carrier number inside the cavity is much larger than the photon number, one may approximately take

$$\delta N_0 = 0 \quad (17c)$$

3. Calculations and discussions

The parameters used in the calculations are $c = 3 \times 10^8$ m/s, $g = 1.1 \times 10^{-12}$ m³/s, $\alpha = 5$, $\tau_s = 2.2$ ns, $\tau_p = 1.6$ ps, $\tau_L = 2n_g L/c$, the cavity length $L = 250$ μ m, the group refractive index $n_g = 4$, $V = 10^{-16}$ m³, $N_p = 3.21 \times 10^{24}$ m⁻³, and $N_{th} = 2.14 \times 10^{24}$ m⁻³ [19, 21]. For a frequency detuning $\Delta\nu$ of -2 GHz ($\Delta\omega = 2\pi\Delta\nu$), to realize an injection-locked operation, the value of the injection coefficient K^2 should be kept within a range from -34.9 dB to -35.8 dB. In the following discussions, the value of K^2 is selected to be -35.2 dB.

3.1. The initial deviations versus θ

The normalized initial deviations $\delta A_0/\delta A_0|_{\max}$ and $\delta\phi_0/\delta\phi_0|_{\max}$ versus θ (from 0 to 360°) are drawn in Fig. 2, where the subscript “max” indicates the maximum achievable δA_0 and $\delta\phi_0$ by one spontaneously emitted photon. From Fig. 2, it can be seen that δA_0 takes a cosine form with respect to θ , while $\delta\phi_0$ takes a sine form. The phase difference between δA_0 and $\delta\phi_0$ is $\pi/2$. These calculated results can be explained by Eqs. (16) and (17).

3.2. Impact of the spontaneously emitted photon on the injection-locked system

When $\theta = 80^\circ$, the corresponding initial deviations are $\delta A_0/A_{st} = 6.235 \times 10^{-4}$, $\delta\phi_0/\phi_{st} = 0.0417$, and $\delta N_0 = 0$. For this case, each deviation and its components versus time are shown in Figs. 3 to 5.

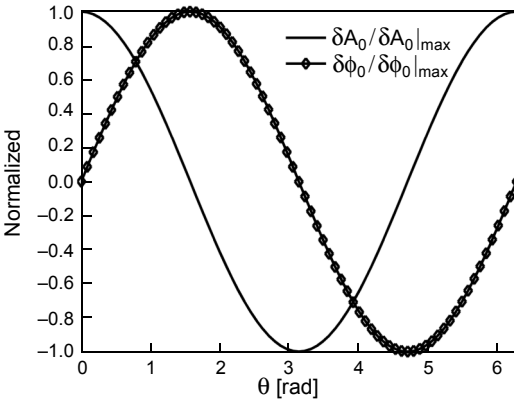


Fig. 2. Normalized initial deviations $\delta A_0/\delta A_0|_{\max}$ and $\delta\phi_0/\delta\phi_0|_{\max}$ versus θ .

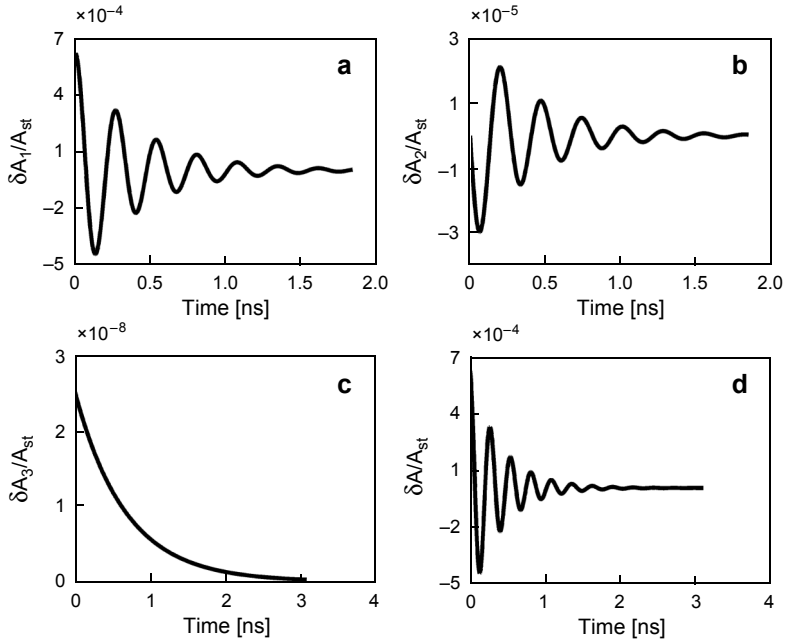


Fig. 3. $\delta A_j/A_{st}$ ($j = 1, 2, 3$) and $\delta A/A_{st}$ versus t .

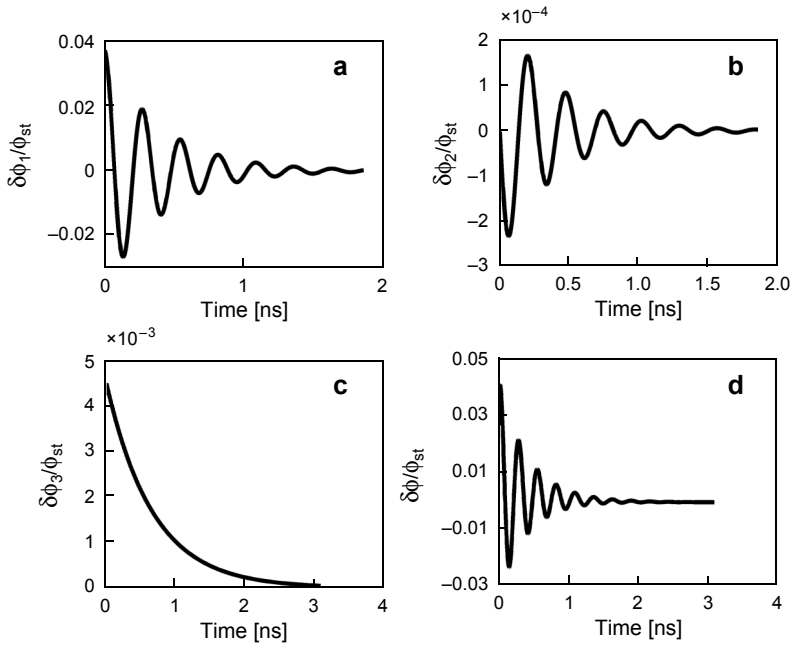


Fig. 4. $\delta\phi_j/\phi_{st}$ ($j = 1, 2, 3$) and $\delta\phi/\phi_{st}$ versus t .

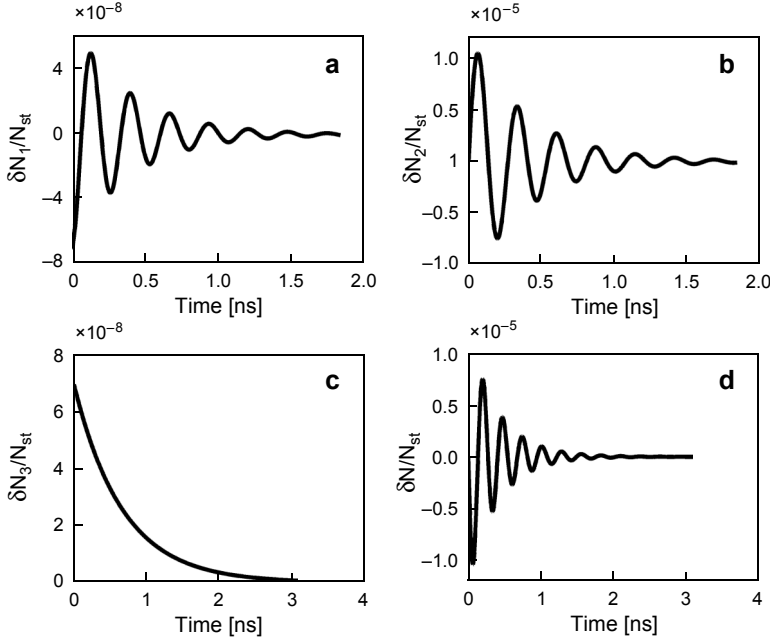


Fig. 5. $\delta N_j/N_{st}$ ($j = 1, 2, 3$) and $\delta N/N_{st}$ versus t .

Compare the subplots (a) and (b) in Figs. 3 to 5, it can be seen that δX_1 and δX_2 ($X = A, \phi, N$) experience damped oscillations, with the same damping time (1.85 ns) and oscillation frequency (3.69 GHz), but with different amplitude and phase (phase difference of $\pi/2$); while $|\delta X_3|$ ($X = A, \phi, N$) monotonously decrease to zero with a decay time of 3.09 ns. In other words, the three deviations δX ($X = A, \phi, N$) include not only damped oscillation parts, but also monotonous decay part. From the calculated results shown in Fig. 5, it can also be seen that, although δN_0 is 0, δN_j ($j = 1, 2, 3$) are not all equal to 0, just the sum of these three components is 0 at the initial moment $t = 0$.

3.3. The phase space portraits with different θ

In this section, we plot the three-dimensional phase space portrait of the SL state from the perturbed initial state to the stable fixed point related to θ in Fig. 6, by using the three time-dependent deviations $\delta A/A_{st}$, $\delta \phi/\phi_{st}$ and $\delta N/N_{st}$.

From Figure 6, it can be observed that, in the phase space, the points representing the state of the SL converge to the stable fixed point in a clockwise spiral pattern. These patterns are independent and disjoint. In Figure 6a, where the angle difference between these two θ is 180° , the initial points have the following relations, $\delta A_0|_{\theta=80^\circ} = -\delta A_0|_{\theta=-100^\circ}$ and $\delta \phi_0|_{\theta=80^\circ} = -\delta \phi_0|_{\theta=-100^\circ}$, that is, the two initial points are center

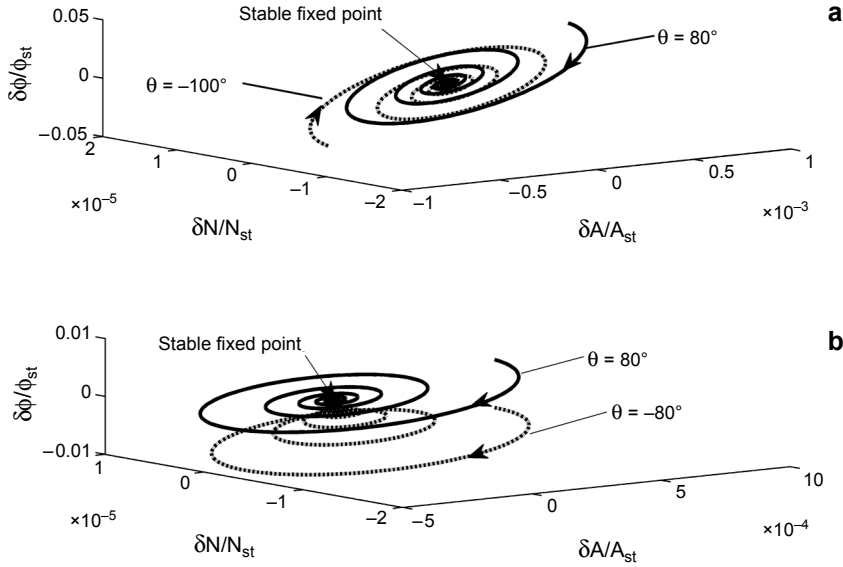


Fig. 6. Phase space portrait of the SL state from the perturbed initial state to the stable fixed point. The arrows point out the spiral direction, and $(0, 0, 0)$ denotes the position of the stable fixed point. $\theta = 80^\circ$ (solid lines) and $\theta = -100^\circ$ (dotted lines) – **a**; $\theta = 80^\circ$ (solid lines) and $\theta = -80^\circ$ (dotted lines) – **b**.

symmetric with respect to the stable fixed point. So they are the phase space portraits. While in Fig. 6**b**, where the angle of these two θ is in reverse, $\delta A_0|_{\theta=80^\circ} = -\delta A_0|_{\theta=-80^\circ}$ and $\delta\phi_0|_{\theta=80^\circ} = -\delta\phi_0|_{\theta=-80^\circ}$. Their phase space portraits are in the same direction with different start points in different plane.

4. Conclusions

The dynamic behaviors of the SL from the initial perturbed state to the fixed point in the disturbed MSLs, which is due to the spontaneously emitted photon, have been analyzed by using the perturbation method and Cardan formula. The calculated results show that the disturbed system will converge to the fixed point in a clockwise spiral pattern. In the process approaching the fixed point, each deviation includes two damped oscillation parts and a monotonous decay part. The damped oscillation parts have the same damping rate and oscillation frequency, but different amplitude and phase (phase difference of $\pi/2$). The phase space portraits with different phase difference between the spontaneously emitted photon and the injection field are in different plane and disjointed.

Acknowledgements – The financial support from the National Natural Science Foundation of China (Grant No. 60890200) is gratefully acknowledged.

References

- [1] LANG R., *Injection locking properties of a semiconductor laser*, IEEE Journal of Quantum Electronics **18**(6), 1982, pp. 976–983.
- [2] BOCHOVE E.J., *Theory of modulation of an injection-locked semiconductor diode laser with applications to laser characterization and communications*, Journal of the Optical Society of America B **14**(9), 1997, pp. 2381–2391.
- [3] LIU J.M., CHEN H.F., MENG X.J., SIMPSON T.B., *Modulation bandwidth, noise, and stability of a semiconductor laser subject to strong injection locking*, IEEE Photonics Technology Letters **9**(10), 1997, pp. 1325–1327.
- [4] VAINIO M., MERIMAA M., NYHOLM K., *Modulation transfer characteristics of injection-locked diode lasers*, Optics Communications **267**(2), 2006, pp. 455–463.
- [5] GAO X., ZHENG Y., KAN H., SHINODA K., *Effective suppression of beam divergence for a high-power laser diode bar by an external-cavity technique*, Optics Letters **29**(4), 2004, pp. 361–363.
- [6] LAU E.K., SUNG H.K., WU M.C., *Scaling of resonance frequency for strong injection-locked lasers*, Optics Letters **32**(23), 2007, pp. 3373–3375.
- [7] LEE E.K., PANG H.S., PARK J.D., LEE H., *Bistability and chaos in an injection-locked semiconductor laser*, Physical Review A **47**(1), 1993, pp. 736–739.
- [8] TAKIGUCHI Y., OHYAGI K., OHTSUBO J., *Bandwidth-enhanced chaos synchronization in strongly injection-locked semiconductor lasers with optical feedback*, Optics Letters **28**(5), 2003, pp. 319–321.
- [9] XIAOFENG LI, WEI PAN, BIN LUO, DONG MA, YONG WANG, NUOHAN LI, *Nonlinear dynamic behaviors of an optically injected vertical-cavity surface-emitting laser*, Chaos, Solitons and Fractals **27**(5), 2006, pp. 1387–1394.
- [10] YUNCAI WANG, GENGWAI ZHANG, ANBANG WANG, *Enhancement of chaotic carrier bandwidth in laser diode transmitter utilizing external light injection*, Optics Communications **277**(1), 2007, pp. 156–160.
- [11] SOMEYA H., OOWADA I., OKUMURA H., KIDA T., UCHIDA A., *Synchronization of bandwidth-enhanced chaos in semiconductor lasers with optical feedback and injection*, Optics Express **17**(22), 2009, pp. 19536–19543.
- [12] HURTADO A., QUIRCE A., VALLE A., PESQUERA L., ADAMS M.J., *Nonlinear dynamics induced by parallel and orthogonal optical injection in 1550 nm vertical-cavity surface-emitting lasers (VCSELs)*, Optics Express **18**(9), 2010, pp. 9423–9428.
- [13] YAN SEN LIN, *Enhancing the relaxation oscillation frequency of a chaotic semiconductor laser transmitter using optical dual-feedback light*, Optics Communications **283**(17), 2010, pp. 3305–3309.
- [14] LIPING ZHANG, RUHAI DOU, JIANGUO CHEN, *Analysis of the phase-locked laser diode array with an external cavity*, Semiconductor Science and Technology **22**(12), 2007, pp. 1253–1257.
- [15] TOOMEY J.P., KANE D.M., DAVIDOVIC A., HUNTINGTON E.H., *Hybrid electronic/optical synchronized chaos communication system*, Optics Express **17**(9), 2009, pp. 7556–7561.
- [16] ZHAO Q., WANG Y., WANG A., *Eavesdropping in chaotic optical communication using the feedback length of an external-cavity laser as a key*, Applied Optics **48**(18), 2009, pp. 3515–3520.
- [17] ARGYRIS A., BOGRIS A., HAMACHER M., SYVRIDIS D., *Experimental evaluation of subcarrier modulation in chaotic optical communication systems*, Optics Letters **35**(2), 2010, pp. 199–201.
- [18] KADDOUM G., COULON M., ROVIRAS D., CHARGÉ P., *Theoretical performance for asynchronous multi-user chaos-based communication systems on fading channels*, Signal Processing **90**(11), 2010, pp. 2923–2933.
- [19] VAN TARTWIJK G.H.M., AGRAWAL G.P., *Laser instabilities: A modern perspective*, Progress in Quantum Electronics **22**(2), 1998, pp. 43–122.

- [20] AGRAWAL G.P., DUTTA N.K., *Semiconductor Lasers*, 2nd Edition, Van Nostrand Reinhold, New York, 1993, pp. 238–241.
- [21] MOGENSEN F., OLESEN H., JACOBSEN G., *Locking conditions and stability properties for a semiconductor laser with external light injection*, IEEE Journal of Quantum Electronics **21**(7), 1985, pp. 784–793.

*Received August 17, 2010
in revised form November 16, 2010*